

# Strategies for reducing crosstalk in CNT interconnects

P. S. MALLICK AND P. UMA SATHYAKAM

School of Electrical Engineering

VIT University

Vellore, Tamil Nadu, 632014

INDIA

[psmallick@vit.ac.in](mailto:psmallick@vit.ac.in); [umasathyakam.p@vit.ac.in](mailto:umasathyakam.p@vit.ac.in)

*Abstract:* - This paper presents reduction of crosstalk in CNT bundle interconnects using different innovative strategies. First, we propose the use of semiconducting CNTs (s-CNTs) as electromagnetic interference (EMI) shields for CNT bundle interconnects. We compute the coupling capacitance of the proposed CNT bundle structure which shows that the crosstalk can be reduced significantly by using s-CNTs. Next, we propose a novel geometry for CNT bundles that can reduce the coupling between adjacent CNT bundle interconnects. The proposed geometry can make CNT interconnects perform 46% better in terms of crosstalk induced delay than traditionally proposed square CNT bundles.

*Key-Words:* - carbon nanotubes, interconnects, crosstalk, delay, VLSI, integrated circuits.

## 1 Introduction

The last 10 years have seen a tremendous research and development of on-chip VLSI interconnects for nanoscale technology nodes [1, 2]. This is powered by the discovery of carbon nanotubes which are excellent conductors of both heat and electricity [2]. Currently manufactured ICs have copper interconnects for carrying signals in them. However, in an effort to keep-up with the Moore's law, IC researchers and engineers are now forced to look at alternate interconnect materials like carbon nanotubes [3] because, copper has reached its downsizing limits and leads to reliability problems in future ICs which are fabricated at sub-10nm node size.

Carbon nanotubes are one dimensional quantum wires that can carry current at very high speeds, when used as interconnects in ULSI chips. Research efforts in this direction started from late 2000s onwards [4-7]. However, recent research findings in this field shows that CNT bundle interconnects can suffer from crosstalk and hence, induced delay [8-11, 20]. Many researchers have attempted to reduce this crosstalk by reducing the width or the height of the CNT bundles [12]. This can be possible up to a certain extent. At very small dimensions, it is very difficult to precisely grow and align such small interconnect structures.

Another group has focused on using different arrangements of single walled CNTs (SWCNTs) and multi walled CNTs (MWCNTs) in the interconnect bundle to reduce crosstalk [12, 13]. However, it is highly difficult to realize such CNT

bundle structures in a fabrication facility. At nanoscale dimensions, the interconnect spacing and the dielectric insulators used, play a major role in determining the electrostatic coupling between adjacent wires [12, 19]. So, it gradually becomes difficult to reduce the wire spacing to a few nanometers. Also, integrating dielectric materials that have very small dielectric constant is costly as well as challenging.

So, in this paper, we propose new strategies that are feasible and can be implemented with lesser complexity to reduce the crosstalk in CNT interconnects. The first idea is to use small diameter semiconducting carbon nanotubes as an outer shield to CNT interconnects [14, 18]. Semiconducting CNTs (s-CNTs), that have band gaps ranging from 1 to 2eV, naturally do not conduct the input current. Further, we show that semiconducting CNTs are less polarizable than metallic CNTs (m-CNTs) and they have a smaller dielectric constants ranging from 1.5 to 2 which is comparable to other low-k dielectric materials. So, s-CNTs can be an ideal choice as an EMI shielding material for CNT interconnects.

Secondly, we take advantage of the fact that single walled CNT bundles when arranged in a specific geometry, can reduce the coupling capacitance between the adjacent CNT bundles so that the crosstalk is minimized and hence, signals can propagate faster.

The rest of the paper is organized as follows: in Section 2, we describe the role played by s-CNTs to reduce crosstalk in CNT interconnects. For that, we describe the polarizability and the dielectric constant

models of s-CNTs. Also, the process steps that are needed to integrate s-CNTs into CNT bundle interconnects is explained in detail. Section 3 shows the CNT bundle geometry model that we use to reduce the coupling capacitance and hence, crosstalk in CNT bundle interconnects. Results and discussions are included in both sections. Section 4 concludes the paper.

## 2 Semiconducting CNTs in Crosstalk Reduction

Carbon nanotubes, depend on the way they are rolled-up which can be metallic or semiconducting. Those CNTs that are metallic have a zero bandgap while semiconducting CNTs have band-gaps ranging from 0.2 to 8.0eV. Of all the CNT configurations of (n, m) defined in the CNT periodic table by Quantum wise [15], one-third are metallic while the rest are semiconducting in nature.

So, in this paper, we consider semiconducting CNTs, that are zig-zag ( $n \neq m$ ). We are not considering other chiral CNTs as they have very small band-gaps and hence, may conduct current at high temperatures. Fig. 1 shows the schematic representation of s-CNTs surrounding metallic CNT bundle interconnect.

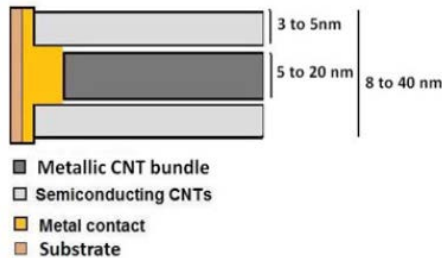


Fig.1 Schematic of proposed geometry of the CNT bundle interconnect with nominal dimensions [14].

The nominal dimensions of the bundle can range from 5 to 20nm while the s-CNT shield can be 2-5nm thick. The overall bundle thickness can be 8 to 40nm. When s-CNTs are used as EMI shields, their radial cross section is exposed to the radiation. So, small diameter s-CNTs, are least polarizable radially and hence, they can have very small dielectric constants of the order of 1.2 to 2.4. The radial polarizability tensor  $\alpha_{\perp}^b$  for a bundle of CNTs of cross sectional area  $\Omega = L^2$  is given as [16]

$$\alpha_{\perp}^b = \frac{\Omega}{4\pi} (\epsilon_{\perp} - 1) \quad (1)$$

where,  $\epsilon$  is the radial dielectric constant and

$$\alpha_{\perp} = \frac{\Omega}{2\pi} \frac{\epsilon_{\perp} - 1}{\epsilon_{\perp} + 1} = \frac{\alpha_{\perp}^b}{1 + \frac{2\pi}{\Omega} \alpha_{\perp}^b} \quad (2)$$

The above expressed polarizability is the unscreened polarizability which arises due to the non-interacting single particle excitations. The screened polarizability of a perfect solid cylinder of radius  $R$  is given by [16]

$$\alpha_{\perp} = \frac{\epsilon - 1}{\epsilon + 1} R^2 \quad (3)$$

From the above equation (3), we compute the radial dielectric constants of small diameter s-CNTs and list them in Table 1.

It must be noted that we propose a stepped CNT bundle contact where the driver of the interconnect is connected to only the inner metallic CNTs, while the peripheral s-CNTs must be electrically inactive. The metal contact must be formed such that the central part of the contact contains more metal atoms (thicker) compared to the peripheral part. For 14 nm technology, we consider the nominal dimensions of the interconnect as shown in Fig. 1.

Table 1 Radial dielectric constants of various s-CNTs (present work)

s-CNT type (n, m)	Radial dielectric constant ( $\alpha_{\perp}$ )
(1,0)	1.46
(2,0)	2.24
(2,1)	2.76
(3,1)	3.24

A mask should be applied to the peripheral part of the contact before m-CNTs are grown at the center. After that, by removing the mask from the contact and masking the m-CNTs, s-CNTs can be grown at the periphery. Chemical mechanical polishing ensures highly oriented and dense bundles after mask removal.

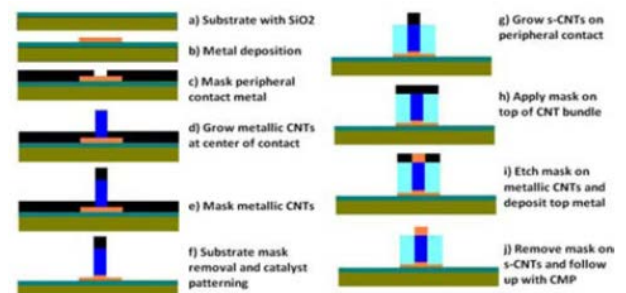


Fig.2 Process steps involved for the proposed CNT interconnect [14].

This process is applicable for both vertical and horizontal interconnects. The schematic of the process steps involved in fabricating the proposed interconnect is shown in Fig. 2.

### 2.1 Results and Discussions

We have analyzed the effect of s-CNTs at the periphery of the CNT interconnects by calculating the coupling capacitance  $C_C$  of the proposed structure, when another CNT interconnect is placed adjacent to it. This coupling capacitance is given by

$$C_C = \frac{\pi\epsilon}{\ln\left(\frac{D}{2(r-d)} + \sqrt{\frac{D^2}{4(r-d)^2} - 1}\right)} F/\mu m \quad (4)$$

where,  $r$  is the radius of the CNT interconnect,  $d$  is the thickness of the s-CNT layer surrounding the interconnect,  $D$  is the distance of separation between adjacent interconnects. The calculated values of the coupling capacitance by varying both  $r$  and  $d$  are shown in Fig. 3.

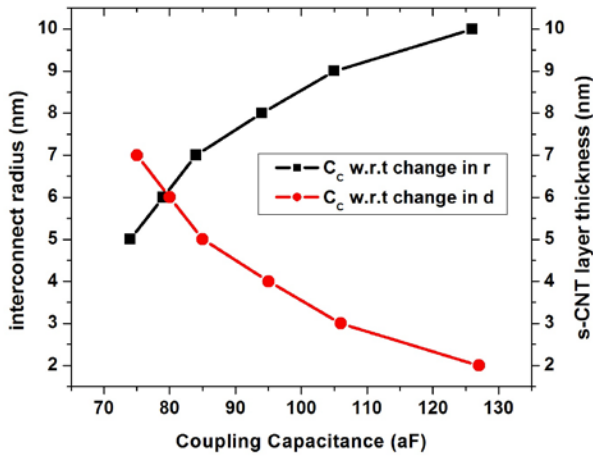


Fig.3 Variation of capacitance with increase in thickness of the s-CNT layer and wire radius for different s-CNT layer thicknesses.

It can be observed that the coupling capacitance increases as the interconnect radius increases while it decreases as the s-CNT layer thickness increases.

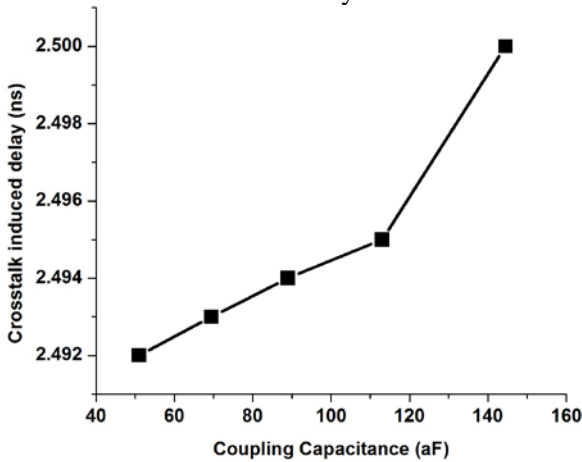


Fig.4 Crosstalk induced delay for different coupling capacitance values, when s-CNTs are used.

Figure 4 shows the crosstalk induced delay which decreases with increase in the coupling capacitance when s-CNTs are used. However, we observed that the crosstalk induced delay is 10 times higher if s-CNTs are not used as EMI shields.

### 3 Geometry Based Crosstalk Reduction Method

Another way to reduce crosstalk in CNT bundle interconnects is by changing the shape of the bundle in such a fashion that least number of CNTs are coupled to each other. Lesser coupling between adjacent CNTs can be achieved only by increasing the distance between them. So, after careful analysis, we came up with a triangular cross sectioned CNT bundle geometry as shown in Fig. 5. As can be observed, the coupling between two triangular CNT bundle interconnects will be the least, when compared to any other possible geometry of the bundle like square, rectangular, hexagonal, circular and so on.

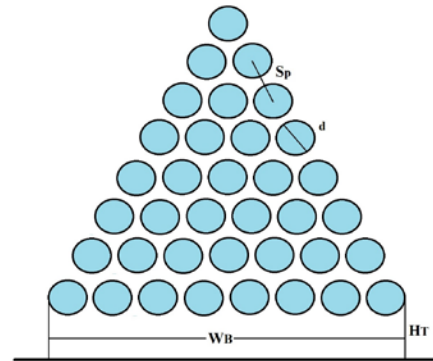


Fig.5 Geometry of Triangular CNT bundle interconnect placed on a grounded plane.

The triangular CNT (T-CNT) bundle has total number of CNTs in the bundle given as,

$$n_{TCNT} = \sum_{b=1}^n n_b(b) = \frac{n_b(n_b + 1)}{2} \quad (5)$$

where,  $n_b$  is the no. of CNTs at the base of the bundle. We consider the T-CNT bundle with  $W_B = 34nm$  with 300 CNTs in it.

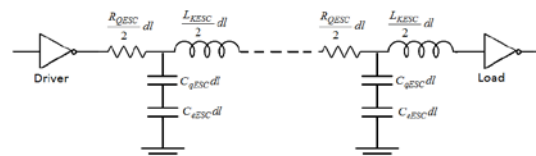


Fig. 6 ESC circuit model of CNT bundle interconnects.

The interconnects are treated as transmission lines (TL) of finite length so that they have intrinsic and parasitic  $R$ ,  $L$  and  $C$ . For bundles of CNTs, we

calculate the equivalent single conductor (ESC) TL models as shown in Fig. 6.

### 3.1 Results and Discussions

To analyze the behavior of the proposed CNT bundles, we apply a pulsed voltage of 0.9V, 4μs pulse width, 8μs pulse duration, 0.1μs rise time and fall time to the ESC modeled SPICE circuits. We consider an inverter made of PTM\_HP FinFET 20nm technology models provided by ASU [17] for simulations using HSPICE. The transistor length is considered at 24nm and width at 15nm, which are nominal values. Fig. 7 shows the propagation delay of the proposed T-CNT bundles along with bundle of aspect ratio (AR) = 1, 1.5 and 2.

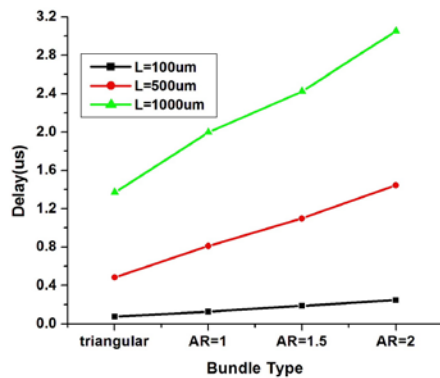


Fig.7 Propagation delay for various bundle types of AR=1, 1.5 and 2 and T-CNT bundle interconnects at various lengths.

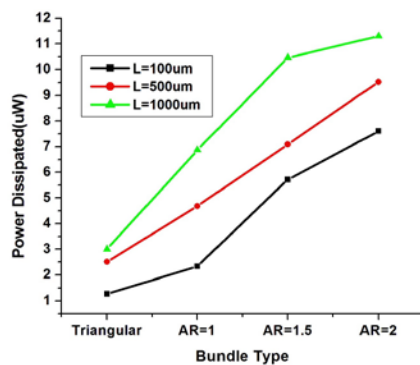


Fig.8 Power dissipated for various bundle types of AR=1, 1.5 and 2 and T-CNT bundle interconnects at various lengths.

Surprisingly, it can be seen that the propagation delay is least for T-CNT bundles compared to bundles of AR=1, 1.5 and 2. From this, we infer that the optimum number of CNTs in a bundle is the same as the number of CNTs in T-CNT bundles that gives optimum delay values for a given length. This is because each CNT contributes to the intrinsic quantum resistance of 6.45kΩ/μm and quantum

capacitance of 400aF/μm. So, in order to achieve minimal delay, both *R* and *C* should be as low as possible. So, typically in our case, the T-CNT bundle quantum capacitance is smaller by 46% compared to AR=1 bundle. Next, we find out the power dissipation by each type of bundles.

From Fig. 8, we can see that the power dissipated by T-CNT bundles is far lesser than its counterparts. When compared to its closest competitor, the power dissipated by T-CNT bundles is 56% lesser than AR=1 bundles at 1000μm. So, this demonstrates the validity and effectiveness of using T-CNT bundles as local, intermediate and global interconnects.

Now, we model the coupling capacitance of T-CNT bundle interconnects when two wires are placed adjacently on a substrate as shown in Fig. 9.

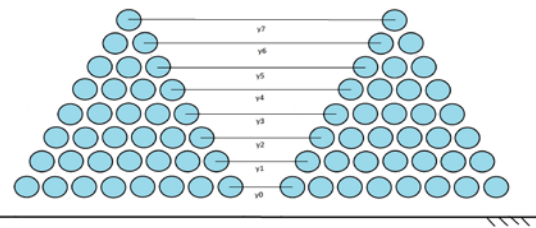


Fig.9 Coupled T-CNT bundle interconnects

So, for two capacitively coupled T- CNT bundles that has *n* number of CNTs along their side, the coupling capacitance of the *n<sup>th</sup>* corresponding CNT pair can be given as

$$C_{C.CNT} = \frac{2\pi\epsilon}{\cosh^{-1} y_n/d} \tag{6}$$

where,  $y_n = y_{n-1} + S_p$  is the inter-CNT distance of the *n*th pair of coupled CNTs,  $n=1,2,3,4,\dots$  and  $y_0 = 34nm$ . So, the total coupling capacitance  $C_C$  of the bundles can be given as

$$C_C = \sum_{m=1}^n C_{C.CNT}^m \tag{7}$$

We compute the  $C_C$  values for T-CNT bundles using (7) and use them in the crosstalk analysis of coupled interconnects.

Next we perform crosstalk analysis of the proposed interconnects when one wire is excited by a pulse signal and another wire is held at logic high. Fig. 10 shows the model of two interconnects placed on a substrate at a distance of  $H_T$  that we use for the analysis. The crosstalk induced delay in the wires will be maximized when the wires are excited with opposite polarity pulses.

However, we are interested in analyzing the performance of T-CNT bundles vs. square bundles. We analyze the impact of increasing the inter-wire distance on the performance of CNT interconnects.

So, we find out the crosstalk induced delay and power dissipation for inter-wire distances of  $S=W$ ,  $S=1.5W$  and  $S=2W$ .

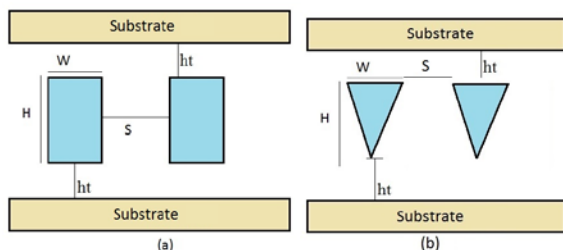


Fig.10 Two coupled (a) square and (b) Triangular CNT bundle interconnects placed on a substrate.

As can be seen from Table 2, the crosstalk induced delay increases for increase in length. Further, as we increase the spacing  $S$ , the delay is reduced. When compared to square bundles, T-CNT bundles have 40%, 41% and 33% reduction in delay for 100, 500 and 1000 $\mu\text{m}$  lengths when  $S=W$ , respectively.

Table 2 Crosstalk induced delay for various wire spacing for triangular and square CNT bundles

Geometry	Length ( $\mu\text{m}$ )	Crosstalk Delay for different interconnect spacing ( $\mu\text{s}$ )		
		$S=W$	$S=1.5W$	$S=2W$
Triangular	100	0.10124	0.10123	0.10122
	500	0.51638	0.5163	0.51627
	1000	1.3881	1.3879	1.3878
Square (AR=1)	100	0.17147	0.17146	0.17144
	500	0.89019	0.89010	0.89004
	1000	2.0941	2.0938	2.0937

Table 3 Power dissipation for various wire spacing for triangular and square CNT bundles

Geometry	Length ( $\mu\text{m}$ )	Power dissipation for different interconnect spacing ( $\mu\text{W}$ )		
		$S=W$	$S=1.5W$	$S=2W$
Triangular	100	0.22515	0.22512	0.2251
	500	1.1308	1.1309	1.1310
	1000	2.1629	2.1626	2.1624
Square (AR=1)	100	0.42441	0.42436	0.42433
	500	2.0706	2.0704	2.0702
	1000	3.8776	3.8772	3.8769

From Table 3, we can see the trend in power dissipation that as the length increases, power dissipation also increases, whereas if we increase the wire spacing, power dissipation decreases.

Moreover, T-CNT bundles dissipate less power than Square bundles. It is 41%, 45% and 44% reduction in power dissipation by T-CNT bundles compared to square bundles at 100, 500 and 1000 $\mu\text{m}$  lengths for  $S=W$ , respectively.

Finally, we compute the power delay product (PDP) which is the ultimate indicator of performance of CNT bundle interconnects. Fig. 11 shows the PDP values at various interconnect lengths for T-CNT bundles and square bundles. It can be seen that, PDP of T-CNT bundles is lesser than square bundles and the difference is more for longer interconnects.

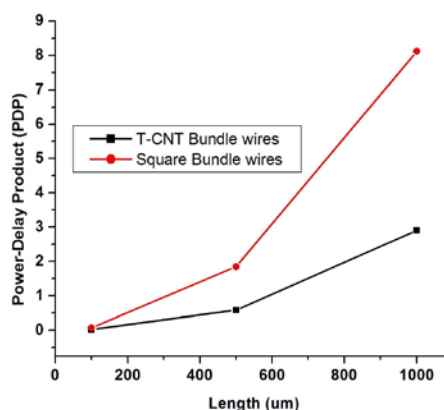


Fig.11 Power Delay Product of T-CNT and Square bundle wires at various lengths.

So, from this analysis, we show that T-CNT bundles, due to their reduced coupling capacitance, perform much better than traditionally used square CNT bundles.

Overall, by comparing the crosstalk and delay reduction for both the strategies mentioned here, we found that using semiconducting CNTs as low-k insulators as well as using of triangular CNT bundles proved to be equally efficient.

### 4 Conclusion

Two strategies are presented in this paper to reduce crosstalk in CNT bundle interconnects. First one is using of semiconducting CNTs as peripheral EMI shield in CNT interconnects and second one is by using triangular CNT bundles. Both methods are more effective in reducing crosstalk and induced delay as compared to conventional methods found in literature. They are also attractive as the design and fabrication complexities can be reduced drastically and hence costs should be lesser to bring the technology to market.

References:

- [1] Y. Awano, S. Sato, M. Nihei, T. Sakai, Y. Ohno and T. Mizutani, Carbon Nanotubes for VLSI: Interconnect and Transistor Applications, *Proceedings of the IEEE*, Vol. 98, No. 12, 2010, pp. 2015-2031.
- [2] M. Shulaker, H.-S. P. Wong and S. Mitra, Computing with Carbon nanotubes, *IEEE Spectrum*, July, 2016, pp. 26-52.
- [3] Ph. Avouris, J. Appenzeller, R. Martel and S. J. Wind, Carbon Nanotube Electronics, *Proceedings of the IEEE*, Vol. 91, No. 11, 2003, pp. 1772-1784.
- [4] A. Naemi and J. D. Meindl, Compact Physical Models for Multiwall Carbon-Nanotube Interconnects, *IEEE Electron Device Letters*, Vol. 27, No. 5, 2006, pp. 338-340.
- [5] A. Nieuwoudt and Y. Massoud, Evaluating the Impact of Resistance in Carbon Nanotube Bundles for VLSI Interconnect Using Diameter-Dependent Modeling Techniques, *IEEE Transactions on Electron Devices*, vol. 53, No. 10, 2006, pp. 2460-2467.
- [6] A. Naemi and J. D. Meindl, Design and Performance Modeling for Single-Walled Carbon Nanotubes as Local, Semiglobal, and Global Interconnects in Gigascale Integrated Systems, *IEEE Transactions on Electron Devices*, Vol. 34, No. 1, 2007, pp. 26-38.
- [7] H. Li, C. Xu, N. Srivastava and K. Banerjee, Carbon Nanomaterials for Next-Generation Interconnects and Passives: Physics, Status, and Prospects, *IEEE Transactions on Electron Devices*, Vol. 56, No. 9, 2009, pp. 1799-1822.
- [8] M. D'Amore, M. S. Sarto, and A. Tamburrano, Fast Transient Analysis of Next-Generation Interconnects Based on Carbon Nanotubes, *IEEE Transactions on Electromagnetic Compatibility*, Vol. 52, No. 2, 2010, pp. 496-504.
- [9] D. Das and H. Rahaman, Analysis of Crosstalk in Single- and Multiwall Carbon Nanotube Interconnects and Its Impact on Gate Oxide Reliability, *IEEE Transactions on Nanotechnology*, Vol. 10, No. 6, 2011, pp. 1362-1371.
- [10] K. Zhang, B. Tian, X. Zhu, F. Wang and J. Wei, Crosstalk analysis of carbon nanotube bundle interconnects, *Nanoscale Research Letters*, Vol. 7, No. 138, 2012.
- [11] P. U. Sathyakam and P. S. Mallick, Towards realisation of mixed carbon nanotube bundles as VLSI interconnects: A review, *Nano Communication Networks*, Vol. 3, No. 3, 2012, pp. 175-182.
- [12] M. K. Majumder, B. K. Kaushik and S. K. Manhas, Analysis of Delay and Dynamic Crosstalk in Bundled Carbon Nanotube Interconnects, *IEEE Transactions on Electromagnetic Compatibility*, Vol. 56, No. 6, 2014, pp. 1666-1674.
- [13] M. K. Majumder, P. K. Das, B. K. Kaushik, Delay and crosstalk reliability issues in mixed MWCNT bundle interconnects, *Microelectronics Reliability*, Vol. 54, 2014, pp. 2570-2577.
- [14] P. U. Sathyakam, A. Karthikeyan and P. S. Mallick, Role of Semiconducting Carbon Nanotubes in Crosstalk Reduction of CNT Interconnects, *IEEE Transactions on Nanotechnology*, Vol. 12, No. 5, 2013, pp. 662-664.
- [15] Periodic Table of CNTs: [Available Online] [https://d3duc685nae4x5.cloudfront.net/documents/CNT\\_PeriodicTable.pdf](https://d3duc685nae4x5.cloudfront.net/documents/CNT_PeriodicTable.pdf)
- [16] B. Kozinsky and N. Marzari, Static dielectric properties of carbon nanotubes from first principles, *Physical Review Letters*, Vol. 96, 2006, pp. 166801.
- [17] Predictive Technology Models: [Available Online] <http://ptm.asu.edu/>
- [18] P. U. Sathyakam, A. Karthikeyan, J. Kavish Rajesh and P. S. Mallick, Reduction of crosstalk in mixed CNT bundle interconnects for high frequency 3D ICs and SoCs, *2014 International Conference on Advances in Electrical Engineering, ICAEE 2014*, Article number 6838461, DOI: 10.1109/ICAEE.2014.6838461
- [19] P. U. Sathyakam and P. S. Mallick, Inter-CNT capacitance in mixed CNT bundle interconnects for VLSI circuits, *International Journal of Electronics*, Vol. 99, No. 10, 2012, pp. 1439-1447.
- [20] A. Karthikeyan and P. S. Mallick, Optimization Techniques for CNT Based VLSI Interconnects-A Review, *Journal of Circuits, Systems and Computers*, Vol. 26, No. 3, 2017, pp. 1730002.